

## Low-field magnetoresistance in tetragonal $\text{La}_{1-x}\text{Ca}_x\text{MnO}_3$ films

J. O'Donnell, M. Onellion, and M. S. Rzchowski

*Department of Physics, University of Wisconsin-Madison, 1150 University Avenue, Madison, Wisconsin 53706*

J. N. Eckstein and I. Bozovic

*Varian Research Center, 3075 Hansen Way, Palo Alto, California 94304*

(Received 13 August 1996; revised manuscript received 17 October 1996)

We have measured the low-field magnetoresistance of molecular-beam-epitaxy-grown tetragonal  $\text{La}_{0.7}\text{Ca}_{0.3}\text{MnO}_3$  films as a function of temperature, and both magnitude and direction of the applied magnetic field. We observed low-field anisotropic hysteresis that depends on the direction of the applied field in the plane of the film. The hysteretic effect can result in a sharp drop in resistance during magnetization reversal which is more than 10 times steeper than the already "colossal" magnetoresistance. We also present evidence of biaxial magnetocrystalline anisotropy with easy axes along the Mn-O bond ( $[100]_t, [010]_t$ ) directions. We show that the low-field anisotropic hysteresis arises from the combined effects of magnetocrystalline anisotropy, anisotropic magnetoresistance, and "colossal" magnetoresistance. Based on a comparison of the data with a simple phenomenological model for the magnetoresistance, we argue that magnetization reversal must proceed by a domain process. [S0163-1829(97)03809-5]

### I. INTRODUCTION

The relationship between the magnetization  $\mathbf{M}$  and resistivity is central to understanding the "colossal" magnetoresistance (CMR) phenomenon in the perovskite manganites. Using applied fields of several Tesla, previous experiments have explored the relation between the magnitude of magnetization and the resistivity, and found the resistivity to be a monotonic decreasing function of  $|\mathbf{M}|$ , quadratic for  $|\mathbf{M}|$  much less than the saturation magnetization  $M_{\text{sat}}$ .<sup>1</sup> In this report we focus on the low-field behavior and find that both the magnitude and direction of the magnetization contribute significantly to the resistivity. We have previously reported evidence for anisotropic magnetoresistance (AMR) in tetragonal  $\text{La}_{0.7}\text{Ca}_{0.3}\text{MnO}_3$  films.<sup>2</sup> This effect, which is a small correction to the CMR at fields on the order of several kOe, manifests itself dramatically in the low-field regime ( $H < 600$  Oe) where it plays a major role in the hysteretic magnetoresistance (MR) which is the subject of this paper. Although hysteretic MR has been observed previously in magnetic materials,<sup>3-5</sup> the MR of those materials is substantially smaller than that of the CMR materials. In this paper, we show that the combined effects of CMR and AMR can increase the low-field sensitivity ( $1/R \, dR/dH$ ) more than tenfold in a narrow field range during magnetization reversal, and that hysteresis in the presence of CMR results in several phenomena which we explore in detail.

Magnetization hysteresis can arise from domain-wall pinning or any of various anisotropies (magnetocrystalline, shape, stress-induced) that cause preferred directions for the magnetization and allow multiple metastable magnetization states at the same applied field.<sup>6</sup> Magnetization hysteresis will then result in MR hysteresis if a magnetoresistance mechanism exists to distinguish the multiple magnetization states. Such a mechanism can be anisotropic magnetoresistance if the multiple magnetization states correspond to different directions for the magnetization, a dependence of the

resistivity  $\rho$  on  $|\mathbf{M}|$  if the multiple magnetization states correspond to different magnitudes of the magnetization, domain-wall scattering or "domain drag"<sup>4</sup> if the multiple magnetization states correspond to the lack or presence of domains, or any combination of these.

In our tetragonal  $\text{La}_{0.7}\text{Ca}_{0.3}\text{MnO}_3$  (LCMO) films the prerequisites for MR hysteresis are present. We have found that the resistivity depends on both the magnitude and direction of the magnetization, and magnetocrystalline anisotropy provides for the possibility of multiple magnetization states at the same applied field. The complex interplay among these effects during the process of magnetization reversal gives rise to diverse behavior in the low-field magnetoresistance.

### II. EXPERIMENTAL PROCEDURE

Our samples are 580 Å thick  $\text{La}_{0.7}\text{Ca}_{0.3}\text{MnO}_3$  films grown by atomic layer by layer molecular-beam epitaxy (ALL-MBE) on  $\text{SrTiO}_3$  substrates. Atomic force microscopy reveals atomically flat terraces interrupted by 4 Å steps in close replication of the substrate with no evidence of grain boundaries or other crystal structure defects. X-ray diffraction data indicate a  $c$ -axis-oriented, tetragonal unit cell ( $a = b = 3.90$  Å,  $c = 3.83$  Å) distorted from the bulk cubic cell. We have presented details of sample growth and morphology elsewhere.<sup>1,2</sup>

The films were patterned into 100  $\mu\text{m}$  wide wires with contact leads suitable for four-terminal resistance measurements. Contact to the patterned leads was made using spring-loaded "pogo" pins. The angular dependence of the MR was investigated by rotating the sample between the pole pieces of a 10 kOe electromagnet which allowed the sample to be rotated 360° while maintaining electrical contact and temperature control. High-field data up to 7 T were taken in a superconducting solenoid. Results for the field applied perpendicular to the substrate have been reported elsewhere.<sup>2</sup>

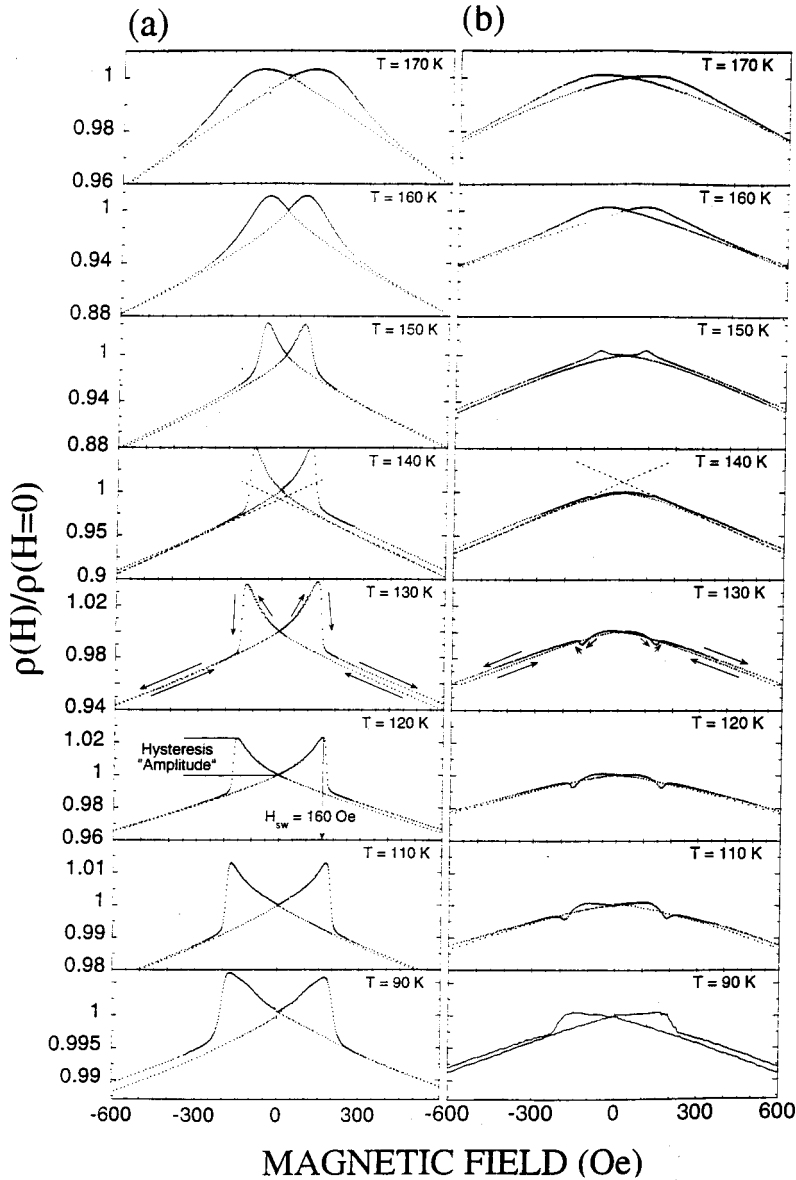


FIG. 1. Normalized resistivity  $\rho(H)/\rho(H=0)$  vs applied field in the plane of the film at a series of temperatures for (a)  $\mathbf{H}\parallel\mathbf{J}$  and (b)  $\mathbf{H}\perp\mathbf{J}$ . Hysteresis loop is traced as indicated by arrows at  $T=130$  K. Also indicated is the “switching” field  $H_{sw}$  and the hysteresis “amplitude.” The linear portion of the 140 K data is extrapolated to emphasize the low-field deviation from linearity. Note the vertical axes are scaled to show the hysteresis clearly.

### III. EXPERIMENTAL RESULTS

The temperature dependence of the resistivity of our samples is similar to earlier reports for thin-film LCMO.<sup>7</sup> Our samples exhibit a resistivity peak at a temperature we label  $T_p$ , usually between 150 and 200 K. Above  $T_p$  the resistivity is accurately described by an activated form with an activation energy of  $\approx 120$  meV. Below  $T_p$  the resistivity drops rapidly with the onset of ferromagnetic order at  $T_c \approx T_p$ . Both above and below  $T_p$  the resistivity is a strong function of the applied field. We refer the reader to Ref. 1 for examples of high-field magnetoresistance and resistivity vs temperature data.

In this section we present experimental evidence that our tetragonal, MBE-grown LCMO films exhibit (a) hysteretic magnetoresistance at low fields, (b) field-direction anisotropy of the hysteretic response, and (c) magnetocrystalline anisotropy. In Sec. IV we show how the CMR, magnetocrystalline anisotropy, and the previously reported anisotropic magnetoresistance<sup>2</sup> combine to give rise to this complex low-field MR hysteresis.

Figure 1 shows the normalized low-field magnetoresistance (MR) at a series of temperatures for a sample with  $T_p = 168$  K. The current density  $\mathbf{J}$  is in the  $[100]$  direction. The applied magnetic field  $\mathbf{H}$  is in the plane of the film either (a) parallel to  $\mathbf{J}$  or (b) perpendicular to  $\mathbf{J}$ . Beginning approximately 10 K above  $T_p$ , careful dc resistivity measurements below 1000 Oe reveal hysteresis in the resistivity  $\rho$  vs  $\mathbf{H}$ . Following the arrows of Fig. 1 at 130 K, upon decreasing  $H$  from +1000 Oe (where the sample is presumed to be single domain) the resistivity is linear in  $H$ . As the field is reduced further the  $\mathbf{H}\parallel\mathbf{J}$  MR begins to deviate superlinearly, while the  $\mathbf{H}\perp\mathbf{J}$  MR deviates sublinearly. The demarcation between the linear and nonlinear behavior is in the range 0–200 Oe, depending on temperature. At negative (reverse biased) fields, the deviation from linearity becomes more severe until beyond a “switching” field  $H_{sw}$  a sharp irreversible drop in resistivity occurs for  $\mathbf{H}\parallel\mathbf{J}$ . The corresponding feature for  $\mathbf{H}\perp\mathbf{J}$  occurs at the same  $H_{sw}$ , but the sharp change is smaller and can be an increase or decrease in resistivity depending on temperature. Tyagi *et al.* have recently reported MR hys-

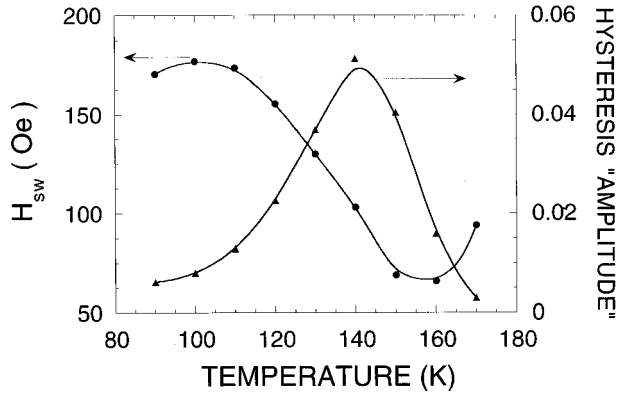


FIG. 2. Characteristic values from Fig. 1, switching field  $H_{sw}$  and hysteresis “amplitude”  $\Delta\rho(H_{sw})/\rho(0)$  vs temperature. The curves are to guide the eye.

teresis in microwave absorption experiments in  $\text{La}_{0.67}\text{Ba}_{0.33}\text{MnO}_3$  films, although they find the effect to be isotropic.<sup>7</sup> Snyder *et al.* have recently reported anisotropic hysteresis in LCMO films grown by metal-organic chemical vapor deposition.<sup>8</sup>

The temperature dependence of the “amplitude” of the hysteretic effect (defined as  $(\rho(H_{sw}) - \rho(0))/\rho(0)$  in Fig. 1(a)), and of  $H_{sw}$  [defined as the field at which the resistivity maximum occurs in Fig. 1(a)] are shown in Fig. 2. As the temperature is decreased below  $T_p$  the “amplitude” of the hysteresis goes through a maximum at 140 K.  $H_{sw}$  monotonically increases with decreasing temperature, consistent with increasing magnetocrystalline anisotropy or domain-wall pinning as we discuss in more detail below. Hysteresis above  $T_p$  indicates the presence of static magnetic order. Similar indications of static (short-range) magnetic order above  $T_p$  have recently been obtained by Oseroff *et al.* in LCMO pellets using electron paramagnetic resonance.<sup>9</sup> Without the ability to probe the magnetization on short length scales ( $\approx 100 \mu$ ) we cannot determine whether the observed hysteresis above  $T_p$  is an intrinsic property, or an artifact due to random sample inhomogeneity.

As seen in Fig. 1 the nature of the MR hysteresis depends strongly on the direction in which the magnetic field is applied. We find that there are two sources of this anisotropy: anisotropic magnetoresistance (dependence of the resistance on the relative angle between the current and the magnetization), and magnetocrystalline anisotropy (preferred directions for the magnetization in the  $a$ - $b$  plane).

At temperatures  $T > 0.8T_p$ , the resistivity in these films has been shown to approximately obey  $\rho(\varphi)/\rho(0) = 1 + b \sin^2 \varphi$  where  $\varphi$  is the angle between the applied field (and by inference the magnetization) and the current.<sup>2</sup> The  $\sin^2 \varphi$  angular dependence is consistent with the anisotropic magnetoresistance (AMR) effect observed in transition-metal ferromagnetic materials.<sup>10</sup> However, the AMR in our LCMO samples differs from that of the transition-metal ferromagnets where the maximum resistance usually occurs when  $\mathbf{H} \parallel \mathbf{J}$ .<sup>11</sup> This corresponds to a negative  $b$ , while for our samples  $b$  is always positive.

At temperatures below approximately  $0.8T_p$ , the AMR deviates from the  $\sin^2 \varphi$  behavior. The origin of this deviation is not yet understood and is the subject of further inves-

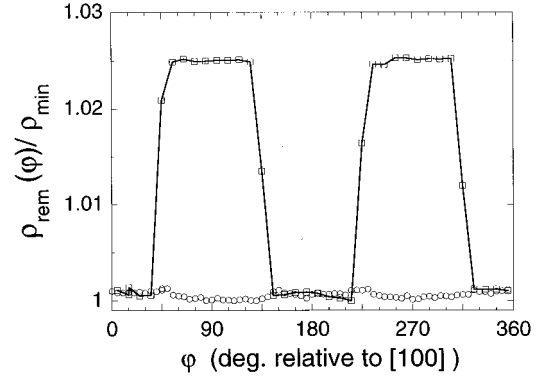


FIG. 3. “Remanent resistivity” at 140 K. Squares indicate the sample with current along [100] ( $T_p = 158$  K). Circles indicate the second sample with current along [110] ( $T_p = 183$  K). Given that both samples exhibit comparable AMR, the angular dependence is consistent with biaxial MCA with [100], [010] easy axes.

tigation. For the purpose of explaining the low-field hysteresis, however, it is sufficient to note that the resistance is maximum when  $\mathbf{M}$  is perpendicular to the current and smaller (though not always a minimum) when  $\mathbf{M}$  is parallel to the current, an observation which is true throughout the entire temperature range.

The final observation necessary to explain the low-field behavior is the existence of magnetocrystalline anisotropy (MCA). To investigate this possibility we compare the “remanent resistivity” of two different samples—one patterned for current flow along the [100] direction, the other for current along [110]. Figure 3 shows the “remanent resistivity” of these two samples. Each data point represents the resistivity in zero applied field after applying a saturating (2 kOe) field at an angle  $\varphi$  relative to [100]. Clearly the [100] sample exhibits two stable remanent resistivities with very few intermediate values. We associate these distinct resistivity values with two distinct magnetic states at  $H=0$ . The transitions between the two states occur at  $\varphi = 45^\circ, 135^\circ, 225^\circ,$  and  $315^\circ$  (relative to the [100] direction) which we interpret as evidence of biaxial MCA in the  $a$ - $b$  plane with easy axes in the [100] and [010] directions. Thus at zero field the magnetization relaxes back to the nearest easy axis with a corresponding resistivity determined by AMR. At temperatures  $T < 0.8T_p$  we find the amplitude of the remanent resistivity vs  $\varphi$  to be consistent with the AMR amplitude indicating the remanent state is essentially single domain. At temperatures near  $T_p$  the remanent resistivity amplitude vanishes (with increasing  $T$ ) faster than the AMR amplitude, and the transitions at  $\varphi = 45^\circ, 135^\circ, 225^\circ, 315^\circ$  become less sharp, suggesting the formation of domains as  $H \rightarrow 0$ .

The situation is much different for the [110] sample. With [100], [010] easy axes, the remanent magnetization lies at  $45^\circ$  relative to the current regardless of the easy axis to which the magnetization has relaxed. Thus the AMR, which depends on the relative angle between  $\mathbf{M}$  and  $\mathbf{J}$ , does not distinguish between different remanent states. The remanent resistivity is therefore independent of the angle of the applied field, in agreement with the inference of biaxial MCA with [100], [010] easy axes drawn from the [100] sample.

#### IV. ANALYSIS

Considering only the CMR of these materials, some features of the MR hysteresis shown in Fig. 1(a) ( $\mathbf{J}$  along  $[100]$ ) can be understood within a simple model. At high positive or negative fields the magnetization is aligned with the applied field. Somewhere in between the magnetization must reverse direction. For a rapid reversal (square magnetization hysteresis loop) one would expect a change in resistivity  $\Delta\rho$  due to CMR of

$$\Delta\rho \approx \rho(M_0 + \chi H_{sw}) - \rho(M_0 - \chi H_{sw}) \quad (1)$$

to accompany the transition of the magnetization from antiparallel ( $M \approx M_0 - \chi H_{sw}$ ) to parallel ( $M \approx M_0 + \chi H_{sw}$ ) to the applied field. Since  $\rho(M)$  is a decreasing function,  $\Delta\rho$  is negative, i.e., a rapid drop in resistivity.  $M_0$  is the spontaneous magnetization, and  $\chi$  is the susceptibility.

This model can explain the rapid decrease in resistivity at  $H = H_{sw}$  for  $\mathbf{H}\parallel\mathbf{J}$ . However, there are several features of the data for which this model cannot account including (a) the deviation from linearity as  $H \rightarrow 0$ , (b) the anisotropy between  $\mathbf{H}\parallel\mathbf{J}$  and  $\mathbf{H}\perp\mathbf{J}$ , and (c) the direction of the irreversible change in resistivity at  $H_{sw}$  for  $\mathbf{H}\perp\mathbf{J}$ . We seek a more detailed model of the magnetization reversal and low-field MR hysteresis which can explain these effects within a single picture.

We first consider the possibility that the sample remains in a single domain magnetic state during the entire magnetization reversal. For such a model (appropriate for a perfect crystal with zero demagnetization field) magnetization reversal by a continuous  $180^\circ$  rotation is not allowed. Rather, there is a ‘‘forbidden band’’ of magnetization directions between the parallel and transverse magnetization states when the field is applied along an easy axis of a crystal with biaxial MCA. (Here ‘‘parallel’’ and ‘‘transverse’’ refers to the direction of the magnetization relative to the applied field.) The magnetization either ‘‘flips’’ directly from antiparallel to parallel alignment as discussed above, or completes the reversal by a two-step process, passing from antiparallel, to transverse, to parallel (see the Appendix). This latter process has been recently observed in  $\text{UFe}_4\text{Al}_8$  single crystals.<sup>12</sup>

Since we have assumed the sample to be a single domain, estimation of the magnetization is particularly easy. When  $\mathbf{M}$  is parallel or antiparallel to the applied field

$$|\mathbf{M}| \approx M_0 \pm \chi H, \quad (2)$$

while for  $\mathbf{M}$  perpendicular to the applied field  $|\mathbf{M}| \approx M_0$  independent of  $H$ . Below  $T_c$ , at the low fields used in this experiment  $\chi H \ll M_0$  for a single-domain particle, and the linear approximation of Eq. (2) is very accurate. Consequently in parallel or antiparallel domains the CMR is also linear in  $H$ . Over the field scale of Fig. 1 the CMR below  $T_c$  is essentially a first-order expansion in the small parameter  $\chi H$  about  $\rho(M_0)$ . As another consequence of linear CMR, the (discontinuous) change in resistivity upon ‘‘flipping’’ of the magnetization from antiparallel to parallel expressed by Eq. (1) is accurately approximated by

$$\Delta\rho = 2\chi H_{sw} \left. \frac{d\rho}{dM} \right|_{M_0}. \quad (3)$$

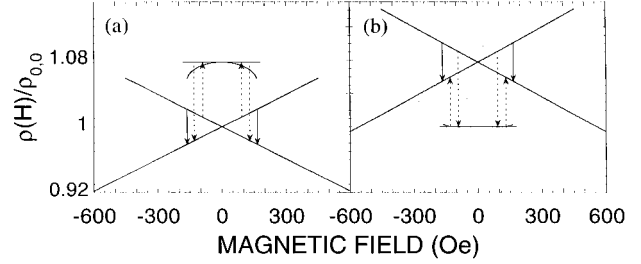


FIG. 4. Calculated resistivity of single domains for (a)  $\mathbf{H}\parallel\mathbf{J}$  and (b)  $\mathbf{H}\perp\mathbf{J}$ . Linear portions represent parallel/antiparallel domains. Constant portion represents transverse domains neglecting rotation of the magnetization. Curved portion represents transverse domains including rotation (see the Appendix). Solid arrows show the transitions in the direct flipping reversal process. Dashed arrows show the transitions in the two-step reversal process.

This is always a drop in resistivity, which is inconsistent with the data of Fig. 1(b).

If the magnetization ‘‘jumps’’ from antiparallel to transverse to parallel in a two-step magnetization reversal, AMR causes the resistivity to change by  $\pm$  the AMR amplitude (depending on the orientation of the field relative to the current). Once in the transverse state, however, the length of the magnetization vector is fixed at  $M_0$ , and the resistivity in the transverse state is independent of applied field. (We are neglecting for the moment the rotation of the magnetization in the transverse domains due to the torque from the applied field, and its effect through AMR on the resistivity.)

Summarizing the MR within the single-domain model: For direct flipping the MR should be linear with a discontinuous drop at  $H_{sw}$  given by Eq. (3) for both  $\mathbf{H}\parallel\mathbf{J}$  and  $\mathbf{H}\perp\mathbf{J}$ . For the two-step reversal process the MR should also be linear, but should show two discontinuous jumps—first up then down for  $\mathbf{H}\parallel\mathbf{J}$  (vice versa for  $\mathbf{H}\perp\mathbf{J}$ ), separated by a region of constant resistivity while the magnetization persists in the transverse orientation. The MR corresponding to these processes is shown in Fig. 4 using the AMR amplitude and CMR sensitivity ( $1/\rho \, d\rho/dH$ ) representative of the data of Fig. 1 at 130 K. Neither discontinuous jumps in resistivity, nor persistence in an intermediate state of constant resistivity are seen in the experimental data of Fig. 1. The single-domain model also fails to predict the deviation from linearity at low fields. We conclude that the single-domain model is inconsistent with the data of Fig. 1.

The shortcomings of the single-domain model can be eliminated with a model postulating a multidomain configuration of the sample. The magnetization reversal then proceeds via motion of domain walls (indicated schematically in Fig. 5), and for applied fields along an easy axis the resistance of the sample is given by

$$\rho \approx x\rho_{\text{par}} + y\rho_{\text{antipar}} + z\rho_{\text{transverse}}, \quad (4)$$

where  $\rho_{\text{par}}$  is the resistivity of domains parallel to the applied field,  $\rho_{\text{antipar}}$  is the resistivity of antiparallel domains,  $\rho_{\text{transverse}}$  is the resistivity of perpendicular domains, and  $x, y, z$  are the fractions of the sample occupied by each domain type.<sup>13</sup>

Within this interpretation the deviation from linearity seen in Fig. 1 is consistent with the nucleation and growth of

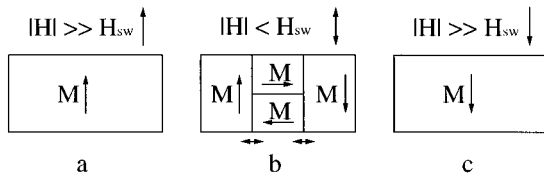


FIG. 5. At fields much greater than  $H_{sw}$  (a),(c) the sample is a single domain. At intermediate fields (b), multiple domains parallel to the easy axes exist in varying abundance determined by  $H$ . As domain walls move, the MR deviates from linearity due to the growth of transverse (to the applied field) domains with higher or lower resistance due to AMR depending on the direction of the current.

transverse domains. For when  $\mathbf{H}\parallel\mathbf{J}$  the magnetization in the nascent transverse domains is perpendicular to the current, and thereby higher in resistivity (due to AMR) giving superlinear deviation as they grow to fill a larger fraction of the sample, while for  $\mathbf{H}\perp\mathbf{J}$  the effect is opposite. To be precise, we must qualify the previous statement. If the CMR sensitivity is very large relative to the AMR amplitude, it is possible for sufficiently large fields that the transverse domains have lower resistivity than the antiparallel domains for  $\mathbf{H}\parallel\mathbf{J}$  (or conversely, higher resistivity than the parallel domains for  $\mathbf{H}\perp\mathbf{J}$ ), i.e., the curves of Fig. 4 can cross. Then the deviation from linearity could be reversed. However, the criterion for this occurring can be shown to be  $(AH_{sw}) > b$  (where  $A = 1/\rho \, d\rho/dH|_{H=500 \text{ Oe}}$  is the normalized CMR sensitivity, and  $b$  is the normalized AMR amplitude). The AMR amplitude  $b$ , and  $(AH_{sw})$  are plotted vs temperature in Fig. 6. Clearly  $(AH_{sw}) \ll b$  at all temperatures, and we are in the limit where the initial growth of transverse domains results in superlinear deviation for  $\mathbf{H}\parallel\mathbf{J}$  and sublinear deviation for  $\mathbf{H}\perp\mathbf{J}$ .

The presence of domains in the sample raises the possibility of domain-wall scattering and/or the ‘‘domain drag’’ effect discussed by Berger.<sup>4</sup> However, these phenomena both increase the resistance leading to superlinear deviation, especially for the  $\mathbf{H}\perp\mathbf{J}$  direction where the domain walls would

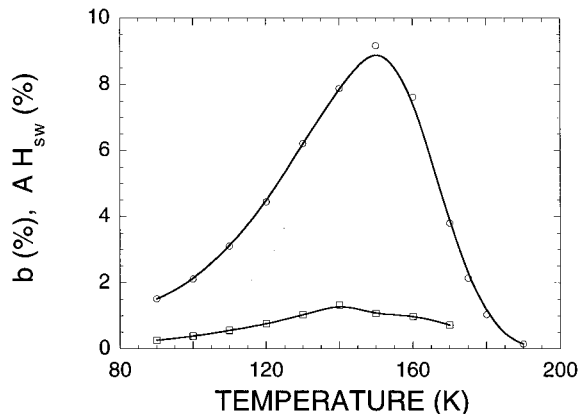


FIG. 6. For the sample of Fig. 1, Circles: AMR amplitude  $b$  (%) plotted vs temperature. Squares:  $AH_{sw}$  ( $A = \text{CMR sensitivity, } 1/\rho \, d\rho/dH$  measured at 500 Oe). Since  $(AH_{sw}) \ll b$ , growth of transverse domains results in deviation from linearity consistent with Fig. 1. The curves are to guide the eye.

likely be perpendicular to the current and the effect greatest. Since we see a sublinear deviation in the  $\mathbf{H}\perp\mathbf{J}$  data, we conclude that domain-wall scattering and/or ‘‘domain drag’’ is a small effect relative to the changes in resistivity due to AMR and domain growth. The fact that the deviation from linearity at high temperatures begins while the sample is still in the ‘‘forward bias’’ condition is further evidence that the remanent magnetic state is multidomain but hysteretic with the dominant domain orientation along the easy axis closest to the most recent saturation direction.

In addition to explaining the curvature of Fig. 1, domain effects also give a consistent explanation of the direction of the sharp change in resistivity at  $H_{sw}$  associated with the final step of magnetization reversal. For  $\mathbf{H}\parallel\mathbf{J}$ , this irreversible resistivity drop can be explained by a rapid growth of aligned domains at the expense of transverse and antiparallel domains. This transition is always accompanied by a drop in resistivity since the final state of the transition ( $\mathbf{M}$  and  $\mathbf{H}$  aligned) is the lowest resistivity of all the allowed domain states. For  $\mathbf{H}\perp\mathbf{J}$  the collapse into the aligned magnetic state can cause an increase or decrease in resistivity because the final state of the transition has an intermediate resistivity; less than the antiparallel domains, but greater than the transverse domains. The deciding factors determining the direction of the resistivity change are therefore the relative populations of transverse vs antiparallel domains at the onset of the transition, and the relative values of the AMR amplitude and the CMR sensitivity. If the sample is primarily antiparallel domains at  $H_{sw}$  the magnetization reversal is nearly direct flipping, and will be accompanied by a drop in resistivity as discussed above. If transverse domains are abundant at  $H_{sw}$  the final collapse into the parallel state will be accompanied by an increase in resistivity. Both behaviors are seen in Fig. 1(b).

In the above analysis we have shown the MR of Fig. 1 to be consistent with magnetization reversal via domain-wall motion with the sample existing in a multidomain state during the reversal process. The mathematical basis for this simple model is given in the Appendix. We have neglected the effect of rotation of the magnetization within transverse domains due to the torque from the applied field which is equivalent to assuming the MCA is very strong. In the Appendix we also consider the effect of rotation of the magnetization within transverse domains. We find this to be a small correction to the analysis given above, and to not substantially alter the conclusions reached disregarding this effect.

In order to reach the conclusion that including rotation is a small correction to the infinite MCA analysis the strength of the MCA must be estimated. Our estimate is based on examining MR hysteresis loops for applied fields at a series of angles in the plane of the film. If the MCA were very strong, the magnetization in a domain would remain closely aligned with the nearest easy axis. Then the component of  $\mathbf{H}$  along  $\mathbf{M}$  (and therefore  $dM/dH$ ) would be reduced by a factor  $\cos(\varphi - \theta)$  where  $\varphi - \theta$  is the angle between  $\mathbf{H}$  and  $\mathbf{M}$ . Since  $d\rho/dH = d\rho/dM \, dM/dH$ , the slope of the MR would also reflect this  $\cos(\varphi - \theta)$  decrease.

Figure 7 shows MR hysteresis loops taken at 140 K with the applied field at a series of angles in the film plane. The fact that the slopes of all these curves are approximately the same for fields greater than approximately 600 Oe indicates

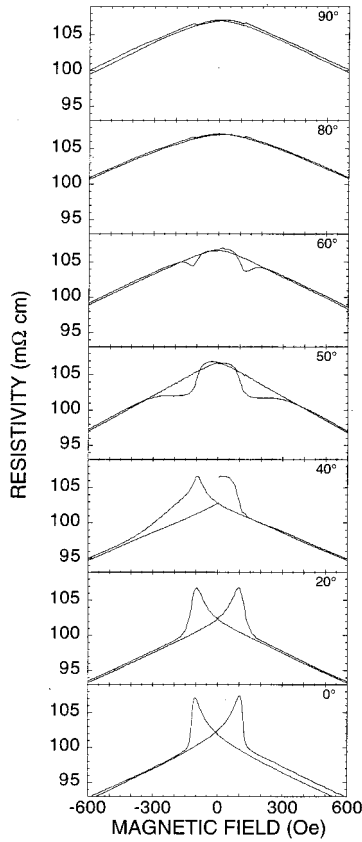


FIG. 7.  $\rho$  vs  $H$  at 140 K of the sample of Fig. 1 for a series of applied field angles. Outside the hysteretic region the slopes are approximately the same indicating substantial magnetization rotation.

that the magnetization must be closely aligned with the applied field (i.e.,  $\theta \approx \varphi$ —the rotation of the magnetization within domains is substantial at fields on the order of 600 Oe). As shown in the Appendix, complete rotation of the magnetization by fields of approximately 600 Oe puts an upper limit on the strength of the MCA.

## V. SUMMARY

We have presented evidence for magnetocrystalline anisotropy, low-field MR hysteresis, anisotropic magnetoresistance, and CMR in tetragonal  $\text{La}_{0.7}\text{Ca}_{0.3}\text{MnO}_3$  films. We have analyzed the hysteresis seen in Fig. 1 within a single magnetic domain model and found that such a model is inconsistent with our data. By contrast, a model that includes multiple domains accounts qualitatively for the main features of the data, namely (a) the deviation from linearity as  $H \rightarrow 0$ , (b) the anisotropy between  $\mathbf{H} \parallel \mathbf{J}$  and  $\mathbf{H} \perp \mathbf{J}$ , and (c) the direction of the irreversible change in resistivity at  $H_{sw}$ . All three result from the changing populations of the three domain types (parallel, antiparallel, and transverse) and their influence on the resistivity through AMR and CMR. Domain-wall scattering and/or “domain drag” has been ruled out as a significant contributor to the low-field MR hysteresis. As discussed in the Appendix, our Fig. 7 data allow us to estimate the strength of the MCA (as measured by  $K/M_0$ ). At 140 K we find  $K/M_0$  must be between 190 and 300 Oe.

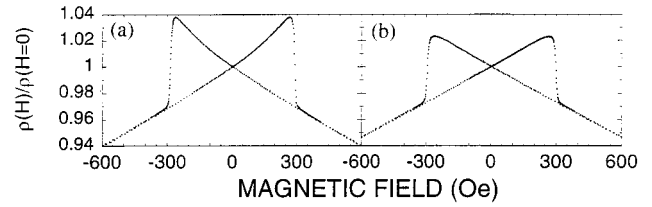


FIG. 8. Low-field hysteresis of the [100] sample of Fig. 3. The sharp drop in resistivity at  $H_{sw}$ , and very little anisotropy between (a)  $\mathbf{H} \parallel \mathbf{J}$  and (b)  $\mathbf{H} \perp \mathbf{J}$  indicates a nearly direct flipping transition with no significant generation of transverse domains.

We have studied several samples, and find that subtle changes of the sample stoichiometry and microstructure can affect the anisotropy. As Fig. 8 illustrates, it is possible to fabricate a sample with very sharp drops in the resistivity at  $H = H_{sw}$ , pronounced hysteresis, but no significant anisotropy between  $\mathbf{H} \parallel \mathbf{J}$  and  $\mathbf{H} \perp \mathbf{J}$ . This sample exhibits MCA (see Fig. 3) and AMR comparable in amplitude to the sample of Fig. 1. The very small anisotropy in the MR hysteresis of this sample can be explained by the relative unimportance of the formation of transverse domains. The magnetization reversal proceeds via nearly direct flipping of the magnetization, or the nucleation and immediate rapid growth of parallel domains. We have achieved a sensitivity  $1/\rho \, d\rho/dH$  at the steepest point of the resistivity drop at  $H_{sw}$  of 0.36%/Oe at 100 K in the as-grown film of Fig. 8. With no attempt at optimization, this compares well to sensitivities reported for tailored giant magnetoresistance heterostructures of approximately 1.5%/Oe.<sup>14</sup>

## ACKNOWLEDGMENTS

This work is supported by the Office of Naval Research through Contracts No. N00014-940-C-0011 and N00014-94-1-0237 and the National Science Foundation through Award No. DMR-96-32527.

## APPENDIX: MAGNETORESISTANCE AND MAGNETIZATION REVERSAL IN THE PRESENCE OF MAGNETOCRYSTALLINE ANISOTROPY

To analyze the MR of single-domain states as discussed above, we have developed a phenomenological model which incorporates the effects of finite MCA. That is, rotation of the magnetization within transverse domains due to the torque from the applied field is included.

As stated in Sec. IV, the CMR below  $T_c$  is linear in the low-field regime of Fig. 1. We assume that the AMR alters the resistivity by a multiplicative factor  $(1 + b \sin^2 \theta)$  with  $b$  independent of  $H$ .<sup>2</sup> Here  $\theta$  is the angle of the magnetization relative to the current which flows along [100]. Thus the resistivity within a domain can be approximated as

$$\frac{\rho(H, \varphi)}{\rho_{0,0}} = \underbrace{[1 - A H \cos(\theta - \varphi)]}_{\text{CMR}} \underbrace{(1 + b \sin^2 \theta)}_{\text{AMR}} \quad (\text{A1})$$

where

$$A \equiv \frac{1}{\rho_{0,0}} \left. \frac{d\rho}{dM} \right|_{M_0} \chi$$

represents the CMR sensitivity, and the  $\cos(\theta-\varphi)$  term expresses the fact that only the component of  $\mathbf{H}$  along  $\mathbf{M}$  increases  $|\mathbf{M}|$ .  $\theta$  is the angle of  $\mathbf{M}$ ,  $\varphi$  is the angle of  $\mathbf{H}$  (both relative to  $[100]$ ),  $\rho_{0,0}$  is the resistivity when  $|\mathbf{M}|=M_0$ , and  $H=\theta=0$  [this is different than  $\rho(0,0)$  which is the resistivity when  $H=\varphi=0$ ].

The remaining task is to compute the direction of  $\mathbf{M}$  for a given  $\mathbf{H}$ . Here MCA plays its role. In the  $a$ - $b$  plane of a tetragonal crystal the lowest-order terms of the thermodynamic potential which depend on the direction of  $\mathbf{M}$  are<sup>15</sup>

$$\Phi = K \sin^2 \theta \cos^2 \theta - \mathbf{M} \cdot \mathbf{H},$$

where  $K$  represents the strength of the MCA. Thus in equilibrium, the magnetization points in a direction  $\theta$  satisfying the following equations which can be solved numerically for any  $H, \varphi$ :

$$\sin 4\theta = 2h \sin(\varphi - \theta), \quad \left( \frac{d\Phi}{d\theta} = 0 \right) \quad (\text{A2})$$

$$\cos 4\theta > \frac{h}{2} \cos(\varphi - \theta) \quad \left( \frac{d^2\Phi}{d\theta^2} > 0 \right). \quad (\text{A3})$$

If  $K > 0$  Eq. (A2) results in easy axes at  $\theta=0^\circ, 90^\circ, 180^\circ, 270^\circ$ , while for  $K < 0$  the easy axes will be along the diagonals in the  $a$ - $b$  plane. We have assumed that for the purpose of determining  $\theta$  the dependence of  $|\mathbf{M}|$  on  $\mathbf{H}$  can be neglected, i.e.,  $|\mathbf{M}| \approx M_0$ , and introduced the dimensionless variable

$$h \equiv \frac{|\mathbf{H}|}{K/M_0}.$$

Solving Eqs. (A2) and (A3) for  $\theta(h)$  with  $\varphi=0$  or  $90^\circ$  gives the following results. At  $h=0$ ,  $\theta=0^\circ, 90^\circ, 180^\circ, 270^\circ$  are degenerate solutions. In the range  $0 < h < 0.54$  the domain most closely aligned with the applied field is the lowest energy solution, while three other metastable solutions exist. At  $h=0.54$ , the magnetization in transverse domains has reached its maximum rotation of  $\approx 24^\circ$  from the easy axis.<sup>16</sup> Exceeding  $h=0.54$  causes the disappearance of the transverse domain solution. For  $0.54 < h < 2$ , two solutions are possible, one parallel to the applied field and stable, one antiparallel and metastable. Once  $h > 2$  the only solution is for the magnetization parallel to the applied field ( $\theta=\varphi$ ).

To compute the MR corresponding to the transverse magnetization states we can use CMR and AMR parameters at 140 K ( $A=1.3 \times 10^{-4} \text{ Oe}^{-1}$ ,  $b=0.078$ ). The strength of the MCA (which sets the field scale for rotation) is unknown, but we do know  $K/M_0$  must be greater than  $H_{\text{sw}}/0.54 \approx 190 \text{ Oe}$  since we believe that transverse domains exist at least up to  $H_{\text{sw}}$ . But as discussed in Sec. IV, Fig. 7 indicates that magnetization rotation is essentially complete at fields of approximately 600 Oe. It can be shown from Eqs. (A2) and (A3) that the condition for complete magnetization rotation ( $\theta=\varphi$ ) for arbitrary  $\varphi$  is  $h > 2$ . Thus  $K/M_0$  must be less than approximately 300 Oe. We have used 300 Oe as a reasonable estimate for  $K/M_0$  at 140 K.

The curved line in Fig. 4 shows the MR for the transverse domain corrected for the effect of rotation. As indicated in the main text, the change in resistivity due to rotation of the magnetization within the transverse domains is a small effect relative to the AMR amplitude, and does not alter the qualitative interpretation of the anisotropic hysteresis of Fig. 1 in terms of domain growth therein given. The model developed in this appendix has the advantage of allowing one to predict the behavior of the MR within domains when the applied field is in an arbitrary direction.

<sup>1</sup>J. O'Donnell *et al.*, Phys. Rev. B **54**, R6841 (1996).

<sup>2</sup>J. N. Eckstein *et al.*, Appl. Phys. Lett. **69**, 1312 (1996).

<sup>3</sup>E. D. Dahlberg, K. Riggs, and G. A. Prinz, J. Appl. Phys. **63**, 4274 (1988).

<sup>4</sup>L. Berger, J. Appl. Phys. **49**, 2156 (1978).

<sup>5</sup>P. P. Freitas and T. S. Plaskett, Phys. Rev. Lett. **64**, 2184 (1990).

<sup>6</sup>B. D. Cullity, *Introduction to Magnetic Materials* (Addison-Wesley, Reading, MA, 1972), pp. 332, 338.

<sup>7</sup>S. D. Tyagi, S. E. Lofland, M. Dominguez, and S. M. Bhagat, Appl. Phys. Lett. **68**, 2893 (1996).

<sup>8</sup>G. J. Snyder *et al.*, Appl. Phys. Lett. **69**, 4254 (1996).

<sup>9</sup>S. B. Oseroff *et al.*, Phys. Rev. B **53**, 6521 (1996).

<sup>10</sup>I. A. Campbell and A. Fert, in *Ferromagnetic Materials*, edited

by E. P. Wohlfarth (North-Holland, Amsterdam, 1982), Vol. 3, p. 747.

<sup>11</sup>T. R. McGuire and R. L. Potter, IEEE Trans. Magn. **11**, 1020 (1975).

<sup>12</sup>G. Bonfait *et al.*, Phys. Rev. B **53**, R481 (1996).

<sup>13</sup>Because the resistivity in each type of domain differs only slightly, the geometrical arrangement of the domains gives only a second-order (in  $\Delta\rho/\rho$ ) correction to this expression.

<sup>14</sup>W. Folkerts *et al.*, IEEE Trans. Magn. **30**, 3813 (1994).

<sup>15</sup>L. D. Landau, E. M. Lifshitz, and L. P. Pitaevskii, *Electrodynamics of Continuous Media*, 2nd ed. (Butterworth-Heinemann, Oxford, 1984), p. 139.

<sup>16</sup>This critical value of  $\theta$  is the solution of  $\tan 4\theta_c = 4 \tan(\theta_c - \pi/2)$ .  $h_c=0.54$  then follows from Eq. (A2).